Reprinted from the

OSA Proceedings on

Picosecond Electronics and Optoelectronics

Edited by T. C. L. Gerhard Sollner and David M. Bloom

Volume 4

Proceedings of the OSA Topical Meeting
on Picosecond Electronics and Optoelectronics,
March 8 – 10, 1989,
Salt Lake City, Utah

Optical Society of America
1816 Jefferson Place, N.W. • Washington, DC 20036

Beams of Terahertz Electromagnetic Pulses

Ch. Fattinger and D. Grischkowsky

IBM Research Division, T. J. Watson Research Center,
Yorktown Heights, New York 10598

ABSTRACT

The generation of diffraction limited beams of single-cycle 0.5 terahertz electromagnetic pulses is described. The beams, centimeters in diameter, have a frequency independent divergence of only 15 mrad and have been propagated distances up to 350 cm. The very high collection efficiency of the optical system used for the generation and the detection of these beams provides exceptionally clean and sensitive reception of the transmitted signal. A spectral characterization of water vapor in the intervening ambient air is also presented.

Integrated-circuit Hertzian dipoles, optoelectronically driven by ultrashort laser pulses, have made it possible to generate subpicosecond transients of electromagnetic radiation. The dipole structures have consisted of photoconductive gaps (1), microscopic dipolar antennas (2), and point sources produced by shorting coplanar transmission lines (3,4). An inherent feature of time dependent dipoles on the surface of a dielectric is that most of the radiated power is emitted into the dielectric and only very little power is radiated into the air (5,6). For Hertzian dipoles (point sources) with dimensions small compared to any of the radiated wavelengths the emitted ultrashort radiation pulse can be collimated using optical techniques: By locating the ultrafast point source at the foci of spherical mirrors or lenses contacted to the backside of the chip, a large fraction of the emitted radiation is captured and can be focused or collimated, providing nearly diffraction-limited imaging of the terahertz radiation (3,4). In addition, the excellent focusing properties preserve the subpicosecond response time of the source. This technique allowed us to produce, for the first time, diffraction limited beams of single-cycle 0.5 terahertz electromagnetic pulses (4). The freely propagating teraHz pulses can be easily measured after propagation distances of several meters using the same optical approach as for their generation: The teraHz radiation is focused on a second integrated-circuit photoconductive gap which is probed by a delayed portion of the laser beam.

The coherent detection of these extremely broadband transients of electromagnetic radiation with subpicosecond time resolution makes this optoelectronic technique an important new tool with many possible applications. The most immediate one is the spectroscopic characterization of materials in the teraHz (far-infrared) regime by time domain spectroscopic techniques (7-9). Here, the measured input and propagated electrical pulses are Fourier analyzed, and because the actual electrical field is measured, both the amplitude and phase of the Fourier components are obtained. Consequently, the frequency dependent absorption and dispersion can be determined for any far-infrared transmitting material. However, the most appropriate use would be time-dependent spectral characterizations after an initiating event.

This application is made feasible by the synchronization between the ultrashort light pulses and the teraHz pulses. A completely different type of application would be ranging measurements with a possible precision of better than 100 microns. The fact that millivolt signals are obtained at receivers, allows for possible remote triggering of devices. Finally, it is clear that these beams have tremendous capacity as a communications channel. Unfortunately, the ubiquitous absorption by water vapor will prevent this use in the atmosphere.

In the following we describe an experiment where the optical collimation technique is used to transmit the teraHz pulses over a distance of 350 cm.

The experimental geometry used to generate the transient electric dipole responsible for the teraHz radiation is illustrated in Fig. 1(a). By photoconductive shorting the charged coplanar transmission line with 70 fsec pulses from a colliding-pulse, mode-locked dye laser, a Hertzian dipole is created between the two lines. The 20-mm-long transmission line consisted of two parallel 5 μm wide, 1 μm thick aluminum lines separated from each other by 15 μm. The line was fabricated on an undoped silicon-on-sapphire (SOS) wafer, which was heavily implanted to ensure the required short carrier lifetime (10). The emission of radiation by the subpicosecond dipole created between the two lines is quite efficient, even though the transmission line structure does not act as an antenna for the radiated pulses. The electrical pulses generated on the transmission line were measured by a fast photoconductive switch, probed by the time delayed monitor beam of the same 70 fsec laser pulses. For short propagation distances (< 300 μm), the electrical pulse coupled to the transmission line has the same time dependence as the transient current between the two lines responsible for the teraHz radiation (11).

The structure shown in Fig. 1b used to detect the teraHz radiation is simply a photoconductive gap of 5 μm spacing and a width of 25 μm. The length of the two aluminum strips forming the gap was 1 mm. This gap was fabricated as above on a separate SOS chip. A current amplifier is connected across the gap as indicated. As the focused radiation pulse hits the detector a transient voltage appears across the gap. The induced voltage is measured by shorting the gap with the 70 fsec laser pulses in the detection beam and measuring the collected charge (current) versus the time delay between the excitation and detection laser pulses.

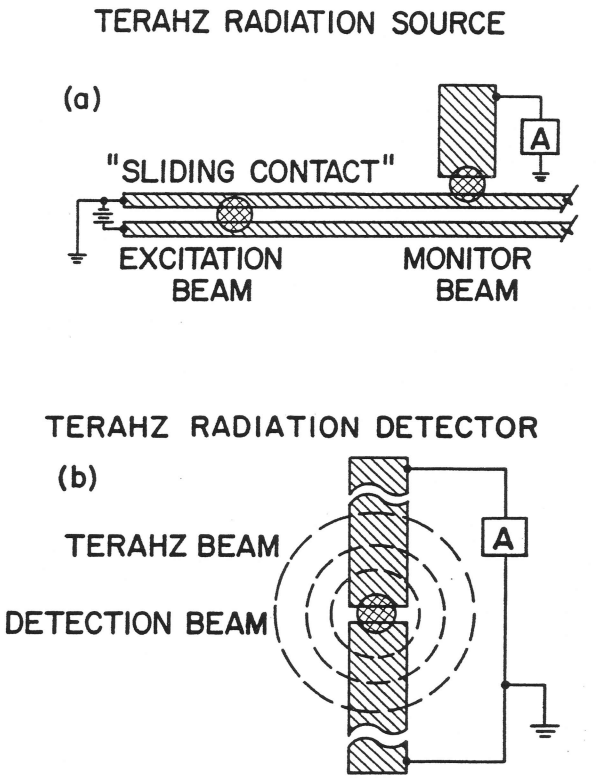

Figure 1. (a) Schematic diagram of the charged coplanar transmission line. The laser excitation beam spot defines the location of the transient electric dipole. The monitor beam measures the electrical pulse coupled to the line. (b) Schematic diagram of the gap detector centered in the concentric focal spots of the incoming teraHz radiation. The laser detection beam spot is centered on the gap.

The teraHz optics at the radiation source and detector consist of two crystalline sapphire, spherical lenses contacted to the backside (sapphire side) of the SOS chips. The center of the two truncated 9.5 mm dia spheres (lenses) is 2.3 mm above the surface of the chips, so that the radiation source and the detector are at the focus of the refracting spherical surface. As shown in Fig. 2 the angular distribution of the power radiated by the dipole on the surface of the chip is drastically effected by the presence of the sapphire/air interface.

Due to the relatively high dielectric constant of 9.6 for sapphire (12), most of the radiation emitted by the ultrafast dipole is contained within a 60 degree full angle cone normal to the surface of the chip and directed into the substrate material (5,6). The boundary of this cone is indicated by the dashed lines in Fig. 2. This situation gives good collection and collimation of the teraHz radiation, because the central portion of the spherical lens captures most of the emission. Taking into account the reflection loss at the surface of the lens we estimate that 30% of the total emitted power is coupled out by the sapphire lens.

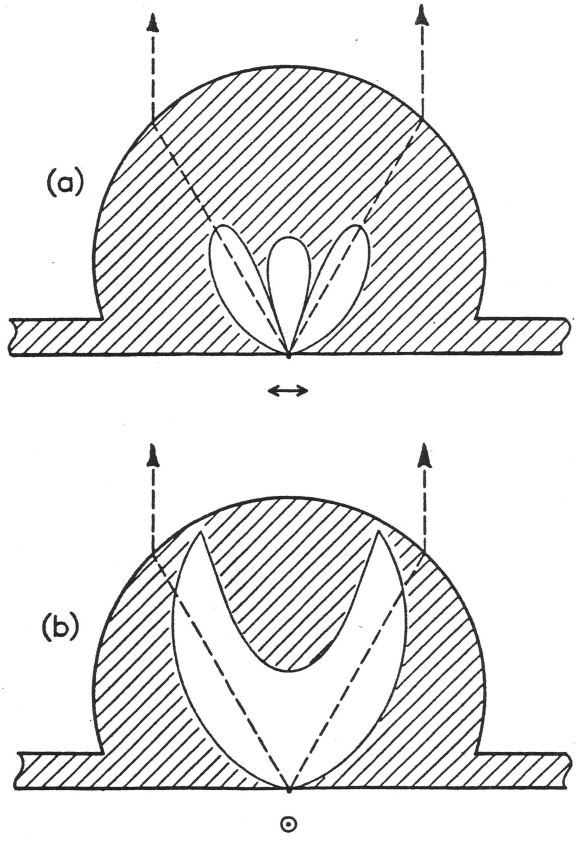

Figure 2. Calculated angular distribution of the power emitted by a Hertzian dipole located on the surface of a dielectric with dielectric constant 9.6. The dipole axis is oriented parallel to the surface. The oscillation of the dipole in (a) is in the plane of the paper, while in (b) the oscillation is perpendicular to (out of) the the plane of the paper. The polar diagrams are shown in orthogonal cross-sections of the sapphire lens. The power emitted into the air is indicated on same scale as the little 'dot' below the focal point of the lens.

After collimation we obtain a beam diameter of 5 mm with a diffraction limited divergence. By reciprocity the emission and detection characteristics of an antenna are identical, and Fig. 2 also applies for the angular dependence of the detection efficiency of the receiving dipole.

It is important to note, that sapphire is strongly birefringent for frequencies in the teraHz range (12). Therefore for both lenses the C-axis of the sapphire was perpendicular to the optical axis of the lens, i.e., parallel to the plane face of the spherical segment. For the source lens and the source chip the C-axes were oriented parallel to the transmission line; for the detecting lens and the detecting chip the C-axes were pependicular to the aluminum strips (parallel to the 25 micron dimension of the gap). Consequently, for both generation and detection the C-axes are perpendicular to the polarization of the teraHz radiation propagating in the direction normal to the surface of the chips. Only for this particular orientation of the C-axes the amplitude of the extraordinary wave cancels at the position of the detector and a clean pulse corresponding to a pure ordinary wave is obtained.

The freely propagating beam pencil, coupled out by the sapphire lens on the source chip, starts out with a frequency independent diameter of about 5 mm, which grows during propagation due to diffraction. As shown in Fig. 3, the diverging beam pencil leaving the sapphire lens can be recollimated with a concave mirror. Our initial set-up is illustrated in Fig. 3a, where the 5 mm diameter diffraction-limited beam from the source lens is emitted at the focal plane of a 25 cm focal-length, spherical, copper mirror with a 50 mm aperture. After recollimation by the mirror, the beam diameter (15-50 mm) is proportional to the wavelength. Therefore the 15 mrad divergence of the collimated beam is the same for all the frequency components in the pulse. The beam then sequentially travels around the numerically indicated rectangular path formed by 4 mirrors of gold coated (1 μm thick) 5.5 cm diameter silicon wafers. The last gold coated mirror (number 4) reflects the beam back to the spherical mirror which then refocuses the beam onto the focusing sapphire lens at the detector. This optical path is equivalent to the simpler schematic diagram of Fig. 3b, where the concentric rings indicate the disc-shaped wave packet associated with the freely

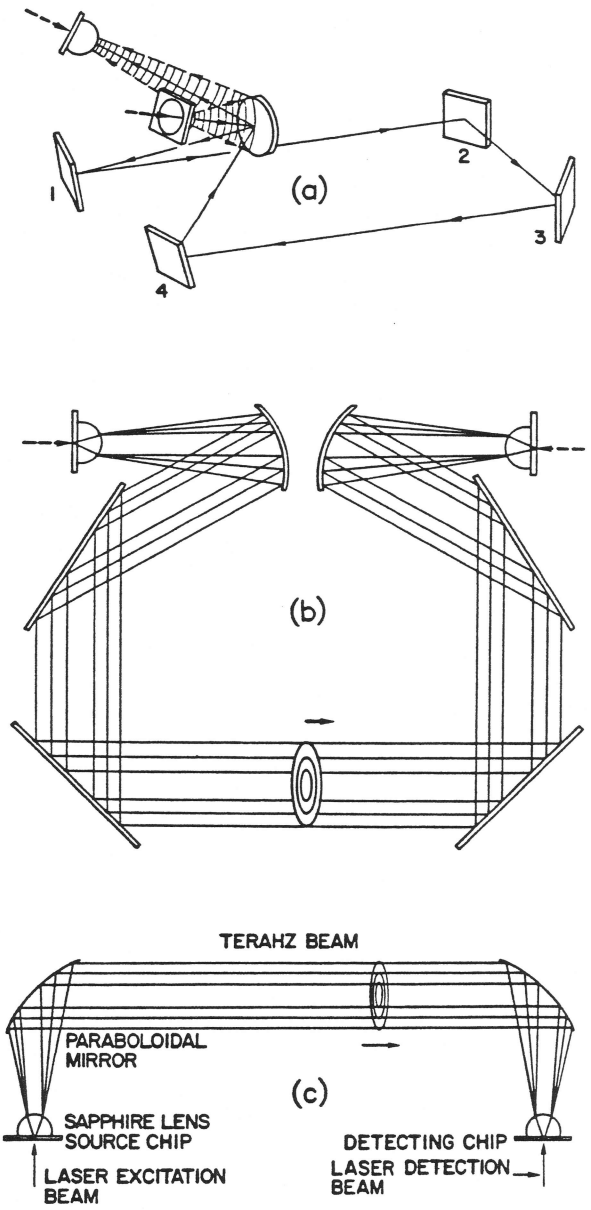

Figure 3. (a) Schematic diagram of the collimating and focusing optics consisting of sapphire lenses in contact with the backside of the SOS chips, located at the focus of a spherical mirror positioned in the center of a delay line defined by 4 flat mirrors. (b) Simplified optical diagram equivalent to (a). (c) Optimal collimating and focusing optics based on paraboloidal mirrors.

propagating teraHz pulse. Inside the smallest ring corresponding to the shortest wavelength, all the frequency components comprising the teraHz pulse are present, and the wave packet has a minimal thickness of only 0.5 mm. After propagating 300 cm to the second identical spherical mirror, the beam is focused on to a second sapphire lens in contact with the detecting chip. Here, all the frequencies are focused to the same 5 mm diameter spot at the entrance to the lens. This lens focuses the beam on to the detection gap, the diameter of the focal spot (200-800 microns) is proportional to the wavelength of the teraHz radiation in sapphire, cf. Fig.1b. The optimal optical arrangement involves the use of paraboloidal mirrors as indicated in Fig. 3c. These mirrors are available commercially in ralatively large diameters. Some of our preliminary results with this arrangement gave excellent collimation and focusing together with no loss in time resolution.

Compared to the previous measurements (4) which used only the sapphire lenses facing each other, the addition of the collimating and focusing mirrors provides a dramatically enhanced coupling between the transmitter and the receiver. Above a certain frequency determined by the acceptance angle (aperture) of the spherical mirrors most of the radiation coupled out by the lens on the source chip is collected and focused back on to the lens on the detecting chip. For the setup described here this critical frequency is 0.25 THz. Because of this very high collection efficiency for frequencies above 0.25 THz the power incident on the detecting chip is about 5% of the power generated by the transmitter.

The generated electrical pulse on the transmission line is shown in Fig. 4a. For this measurement the spatial separation between the sliding contact excitation spot and the monitor gap was 150 microns, so that propagation effects were negligible. The measured full width at half maximum is 0.95 psec. Taking into account the response time of the monitor gap, we consider the actual pulse width of the transient current responsible for the teraHz radiation to be 0.6 psec. Figure 4b is the numerical derivative of the pulse on the line (current pulse) and will be used to calculate the limits of the spectral extend of the resulting radiation pulse.

The energy of the incident 70 fsec laser pulses coming at a 100 MHz rate in a 5 mW

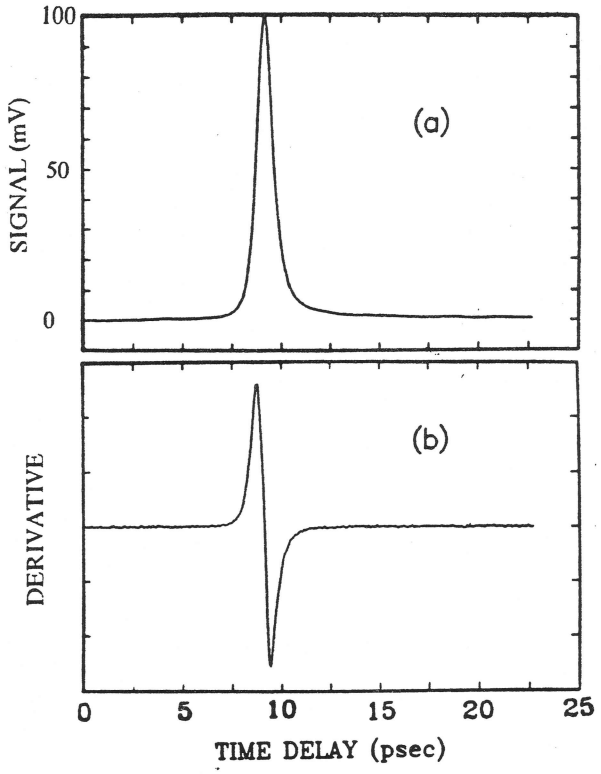

Figure 4. (a) Electrical pulse on the transmission line measured with 150 micron separation between the excitation and monitor beams. (b) Numerical derivative of the measured pulse on the transmission line shown in (a).

beam is 50 picojoules per pulse. With a bias voltage of 20 V, approximately 8000 electrons are transferred between the two lines at the excitation site during one excitation pulse. Knowing this transient current we calculated that 1 attojoule of energy is emitted by the transient dipole moment on the 20 μm wide transmission line (5). Assuming that 20% of the total emitted radiation is found in the freely propagating beam, the resulting energy in the teraHz beam is 0.2 attojoules (approximately 1 eV) per pulse. From the signal strength of 100 mV for the electrical pulse on the coplanar line, knowing that 2 equal and oppositely propagating pulses are generated, and considering the line impedence to be 125 ohms, we calculate approximately 100 attojoules for the electrical pulses coupled to the line. Therefore, the total radiated energy is of the order of 1% of the energy coupled to the transmission line. Another feature is that the conversion of laser energy to electrical pulse energy on the transmission line and to energy in the teraHz beam radiation is a nonlinear process. For example, if the energy in the laser pulse is increased by 10X, the energy in the pulses on the line and in the teraHz radiation increase by 100X.

An important point concerns the extreme sensitivity of the detection technique. The individual teraHz pulses of energy 0.2 attojoules contain approximately 1000 photons. Our measurement system detects these pulses with a signal-to-noise-ratio of 300:1 for an integration time of 0.1 second. Therefore, in terms of minimum detectible energy, we can measure 0.2 attojoules/(90000). This corresponds to a sensitivity of 1/90 photon per pulse. Of course, our repetition rate of 100 MHz, and our gated detection technique are required for this sensitivity. This exceptional sensitivity corresponds to the capability to detect with a signal-to-noise-ratio of 1:1 and for an integration time of 0.1 sec an incoming average power of 0.2 femtoWatts. In comparison a cryogenic bolometer at liquid helium temperature has the sensitivity of 0.1 picoWatt/(square root Hz) (see Ref. 14) corresponding to 150 femtoWatts for a 0.1 sec integration time. The main reason for this exceptional sensitivity of the optoelectronic technique is that the electric field is detected directly and coherently.

Figure 5a shows a previous measurement (4) of the teraHz radiation pulse, obtained without using any mirrors. The main component of the pulse consists of a single cycle of the electromagnetic field with a time duration from maximum to minimum of less than 1 psec. For this measurement the separation between the two sapphire lenses facing each other was 10 cm. Figure 5b displays the detected teraHz radiation pulse after a total propagation distance of 350 cm in air, measured with the set-up illustrated in Fig. 3a. As can be seen, the main component of the signal (Fig. 5b) measured with the 350 cm long complex optical path is similar to the pulse shown in Fig. 5a. However, the oscillations on the trailing edge dramatically increased. These oscillations are due to the water vapor corresponding to a relative humidity of 30%. In order to see the full extent of these oscillations, the length of the scan was increased to 90 psec as shown in Fig. 5c. Here we see that the ringing persists for more than 50 psec.

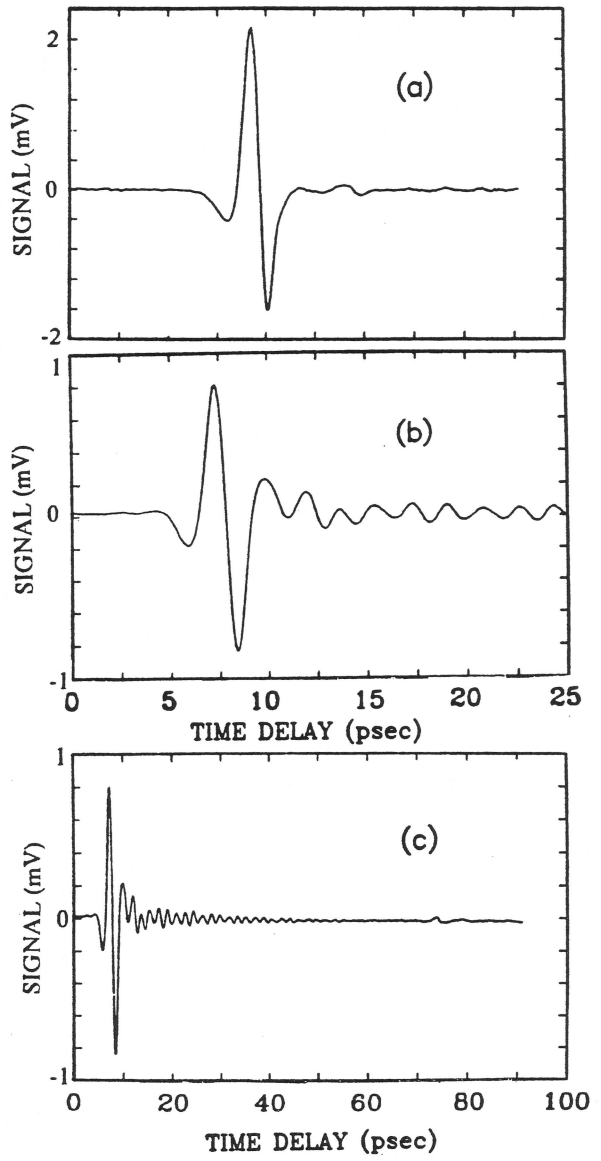

Figure 5. (a) Freely propagating teraHz radiation pulse measured without any mirrors; the separation between the two sapphire lenses facing each other was 10 cm. (b) Radiation pulse of the freely propagating teraHz beam measured with a total propagation path length of 350 cm (cf. Figs. 3a,3b). (c) Longer time scan of (b).

The signal to noise ratio is better than 300:1 for a single 8 min scan of the 90 psec relative time delay between the exciting and probing laser pulses.

The amplitude spectra of the two radiation pulses (Figs. 5a and 5b) are displayed in Figs. 6a and 6b, respectively. Both spectra peak at approximately 0.4 THz. Apart from a modest decrease of the transmitted bandwidth in spectrum 6b compared to spectrum 6a, the two spectra differ by two significant absorption lines of water vapor at 0.56 and 0.75 THz. (The spike at very low frequency is an artifact and can be ignored.) The two observed absorption lines correspond to transitions between rotational modes of the water molecule and are in agreement with earlier measurements (13).

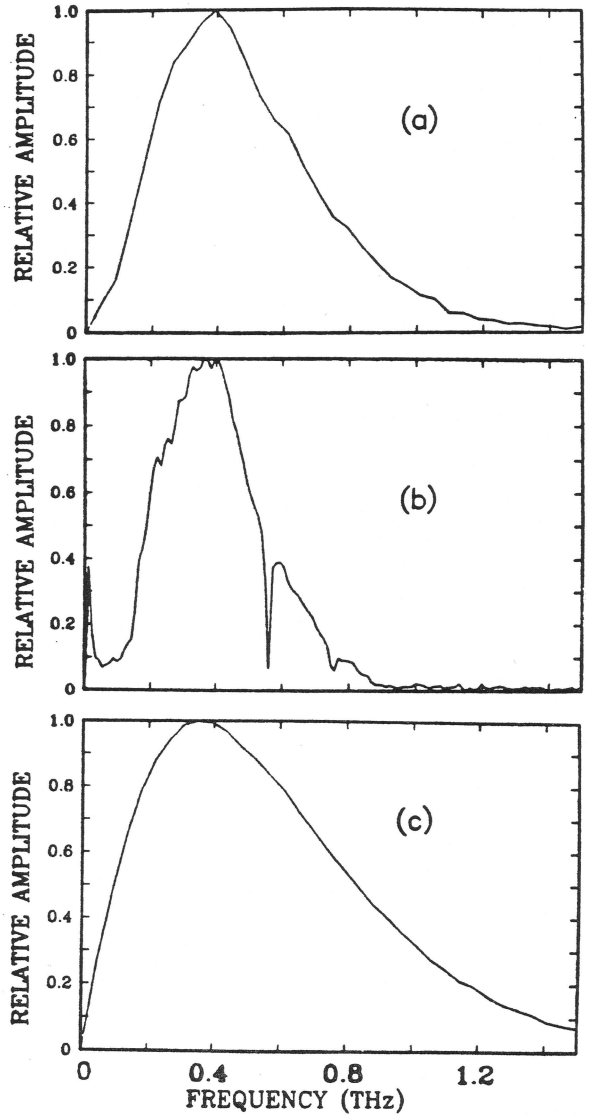

Figure 6. (a) Amplitude spectrum of the pulse shown in Fig. 5a, transmitted over a distance of 10 cm. (b) Amplitude spectrum of the pulse shown in Fig. 5b, transmitted over a total distance of 350 cm. (c) Amplitude spectrum of the numerical derivative of the measured pulse on the transmission line shown in Fig. 4a.

The following argument compares a theoretical lower frequency bandwidth limit for the generated teraHz pulse with the bandwidth of the received signal. In the radiation zone the field of the Hertzian dipole is given by the derivative of the transient current between the two aluminum lines. Figure 4b displays the numerical derivative of the measured electrical pulse on the transmission line shown in Fig. 4a. The amplitude spectrum of this numerical derivative, which is shown in Fig. 6c, provides a lower limit for the true spectral extent of the initially emitted teraHz radiation pulse. This is because the actual transient current at the excitation site is significantly faster than the measured pulse on the transmission line. As can be seen, by comparing Fig. 6c with Figs. 6a and 6b, the lowest and highest frequency components created by the transient dipole on the source chip are not present in the detected radiation pulse. As discussed above, the cut-off for frequency components below 0.25 THz is caused by diffraction.

To explain the observed attenuation of the high frequency components, the following four effects have to be considered: The first and simplest is the frequency dependent reflectivity from the 2 reflections at the copper mirror and the 4 reflections from the gold coated silicon wafers. The second involves the coherent imaging of the teraHz radiation, where wavefront errors due to aberrations of the optical system cause a decrease of the coupling strength between transmitter and receiver. The two off-axis reflections of the THz radiation at the spherical copper mirror induce differences in optical path length between different portions of the beam, which are more severe for the high frequency components of the transmitted signal. The third is the absorption loss in the sapphire lenses which increases with frequency (12). This absorption has a strength such that the total path length of 14mm through the sapphire lenses attenuated the 1 THz component by 1/2. Finally, the 0.8 psec response time of the detector strongly reduces the observed fast time dependence of the received signal.

ACKNOWLEDGMENT

This research was partially supported by the U.S. Office of Naval Research.

REFERENCES

1. D.H. Auston, K.P. Cheung, and P.R. Smith, Appl. Phys. Lett. Vol.45, 284 (1984).
2. P.R. Smith, D.H. Auston, and M.C. Nuss, IEEE J. Quantum Electron. QE-24, 255 (1988).
3. Ch. Fattinger and D. Grischkowsky, Appl. Phys. Lett. Vol.53, 1480 (1988).
4. Ch. Fattinger and D. Grischkowsky, Appl. Phys. Lett. Vol.54, 490 (1989).
5. W. Lukosz and R.E. Kunz, J. Opt. Soc. Am. Vol.67, 1607 (1977), and W. Lukosz, J. Opt. Soc. Am. 69, 1495 (1979).
6. D.B. Rutledge and M.S. Muha, IEEE Trans. Ant. Propagat. AP-30, 535 (1982).
7. D. Grischkowsky, C.-C. Chi, I.N. Duling III, W.J. Gallagher, N.H. Halas, J.-M. Halbout, and M.B. Ketchen, in 'Picosecond Electronics and Optoelectronics II', Proceedings of the Second Topical Conference, Incline Village, Nevada, January 14-16, (1987), Editors, F.J. Leonberger, C.H. Lee, F. Cappasso, and H. Morkoc, (Springer-Verlag, New York 1987).
8. D. Grischkowsky, C.-C. Chi, I.N. Duling III, W.J. Gallagher, M.B. Ketchen, and R. Sprik, 'Laser Spectroscopy VIII', Proceedings of the Eighth International Conference, Are, Sweden, June 22-26, (1987), Editors, W. Persson and S. Svanberg, (Springer-Verlag, New York 1987).
9. Y. Pastol, G. Arjavalingam, J.-M. Halbout, and G.V. Kopcsay, Appl. Phys. Lett. Vol.54, 307 (1989).
10. F.E. Doany, D. Grischkowsky, and C-C. Chi, Appl. Phys. Lett. Vol.50, 460 (1987).
11. D. Grischkowsky, M.B. Ketchen, C-C. Chi, I.N. Duling III, N.J. Halas, J.-M. J-M. Halbout, and P.G. May, IEEE J. Quantum Electron QE-24, 221 (1988).
12. E.E. Russell and E.E. Bell, J. Opt. Soc. Am. Vol.57, 543 (1967).
13. D.E. Burch, J. Opt. Soc. Am. Vol.58, 1383 (1968).
14. C. Johnson, F.J. Low and A.W. Davidson, Optical Engr., Vol. 19, 255 (1980).